

## Active Control of Convection in a Melted Material Layer II. Convection with a Finite Lower Boundary

PhD eng. Maria Neagu  
University "Dunărea de Jos" of Galați

### ABSTRACT

*This paper is the second part of a study of the active control of Bénard-Marangoni convection of an infinite fluid layer with a finite lower boundary. A linear proportional control method is used to perturb the lower boundary heat flux proportional to the local amplitude of a shadowgraph measurement. The influence of the boundary layer properties (thickness, thermal conductivity and diffusivity) on the active control process is analyzed. It is noticed the appearance of an isola, for a certain range of process parameters, as a primary bifurcation towards a time-dependent convection.*

**Keywords:** active control, melted material layer, convection.

### 1. Introduction

Since Pearson [1] proved the phenomenon of surface tension-driven convection and Nield [2] the co-existence of buoyancy and surface tension-driven convection, many researchers studied these phenomena trying to establish clear connection between them. The Rayleigh-Bénard convection and Bénard-Marangoni convection do reinforce each other in the context of the assumption that the upper fluid boundary remains flat [2]. Even if this simplification was already questioned in several studies and Scriven and Sternling [3] concluded that the surface deformability may render the layer of fluid unstable under virtually all conditions, the flat upper boundary condition is an assumption which, used in the theoretical studies of Bénard-Marangoni convection, meets good verification [4-5]. This paper is also considering that the upper surface is flat. For small values of Rayleigh numbers ( $3.0e-7$ ) and thin fluid layers, Bénard-Marangoni convection is responsible for the pattern formation. If the experimental work questioned the stability of patterns which arise and the existence of an unique value for Marangoni number, numerical modeling tried and confirmed the experimental results: the energy stability theory [6], the linear stability analysis [1], [2] and bifurcation analysis [7-8]. This study is a linear stability analysis of a linear proportional method for the active control of Bénard-Marangoni convection.

Rayleigh-Bénard convection and Bénard-

Marangoni convection are not always desired phenomena in industrial applications. The delay or suppress of convection in Rayleigh-Bénard and Bénard-Marangoni convection has received a great attention in the last period [9÷10].

Theoretical studies [11÷14] as well as experimental works [15÷16] analyzed different methods of control of Rayleigh-Bénard convection. The successful results of Tang and Bau [17] initiated the active control of Rayleigh-Bénard convection through the control of temperature or heat flux at the fluid lower boundary. According to the classification established by Gad-el-Hak [18], these are active reactive feedback control methods.

This work is studying the active control of surface tension-induced convection of infinite horizontal fluid layers heated from below with a constant flux, situation which corresponds experimentally to a novel shadowgraphic system.

### 2. Mathematical formulation

For the case of Bénard-Marangoni convection, with the addition of a finite thickness lower boundary, the equation for the perturbation temperature amplitude,  $\Theta$ :

$$\left(D^2 - a^2\right)\left(D^2 - a^2 - \sigma\right)\left(D^2 - a^2 - \frac{\sigma}{Pr}\right)\Theta = -a^2 R\Theta, \quad (1)$$

where  $a$  is the wave number,  $\sigma$  is the growth

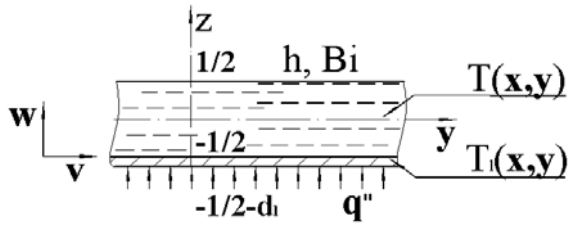


**Fig.1.** Fluid layer with finite lower boundary.

rate,  $R$  is the Rayleigh number,  $Pr$  is the Prandtl number and  $D$  is the notation for  $D = \partial / \partial a$ .

The solution of equation (1) is:

$$\Theta = \sum_{i=1}^3 (E_i \cosh(x_i z) + O_i \sinh(x_i z)) \quad (2)$$

where  $x_i, i=1...3$  are the roots of the characteristic equation:

$$\left(x_i^2 - a^2\right)\left(x_i^2 - a^2 - \sigma\right)\left(x_i^2 - a^2 - \frac{\sigma}{Pr}\right) + a^2 R = 0. \quad (3)$$

The perturbation equation of the lower boundary is:

$$\sigma \theta_1 = \eta (D^2 - a^2) \theta_1, \quad (4)$$

where  $\eta$  is thermal diffusivities ratio of the lower boundary layer and the fluid,  $k_l/k_f$ ; its temperature field is given by:

$$\theta_1 = A \cosh(x_1 z) + B \sinh(x_1 z), \quad (5)$$

where the characteristic value  $x_1$  is the root of the equation:

$$\left(x_1^2 - \frac{\sigma}{\eta}\right) - a^2 = 0. \quad (6)$$

The eight boundary conditions necessary for finding the coefficients  $E_i, O_i, A$  and  $B$ , and, consequently, the perturbation temperature amplitude,  $\Theta$ , are:

- the no penetration condition, applied at upper and lower boundary of the fluid layer,

$$\left(D^2 - a^2 - \sigma\right)\Theta\left(\pm \frac{1}{2}\right) = 0; \quad (7)$$

- the no slip condition, applied at the lower boundary of the fluid layer,

$$M_3 = \begin{bmatrix} 0 & 0 & x_1 S_1 + Bi C_1 & x_2 S_2 + Bi C_2 \\ -x_1 \sinh\left(\frac{x_1}{2} + d_1\right) & x_1 \cosh\left(\frac{x_1}{2} + d_1\right) & -\frac{(2\gamma a^2 \lambda_1) S_1}{x_1} & -\frac{(2\gamma a^2 \lambda_1) S_1}{x_1} \\ \cosh\left(\frac{x_1}{2}\right) & -\sinh\left(\frac{x_1}{2}\right) & -C_1 & -C_2 \\ -x_1 \sinh\left(\frac{x_1}{2}\right) & x_1 \cosh\left(\frac{x_1}{2}\right) & \lambda_1 x_1 C_1 & \lambda_1 x_1 C_1 \end{bmatrix} \quad (15)$$

$$D\left(D^2 - a^2 - \sigma\right)\Theta\left(-\frac{1}{2}\right) = 0; \quad (8)$$

- the thermal transfer condition applied at the upper boundary,

$$D\Theta\left(\frac{1}{2}\right) + Bi\Theta\left(\frac{1}{2}\right) = 0; \quad (9)$$

- the condition of surface-tension driven convection,

$$D^2\left(D^2 - a^2 - \sigma\right)\Theta\left(\frac{1}{2}\right) = a^2 Ma\Theta\left(\frac{1}{2}\right); \quad (10)$$

applied at the upper boundary.  $Bi$  is the Biot number, the Marangoni number

$Ma = \frac{d\gamma_s \bar{q}}{k_f K_f \rho v}$ ,  $d$  is the fluid layer thickness,

$\bar{q}$  is the medium heat flux,  $k_f$  is the fluid thermal diffusivity,  $K_f$  is the fluid thermal conductivity,  $\rho$  is the fluid density,  $v$  is the fluid viscosity and  $\gamma_s$  is thermal coefficient of surface tension.

- the continuity of temperature at the fluid lower boundary,

$$\Theta_1\left(-\frac{1}{2}\right) = \Theta\left(-\frac{1}{2}\right); \quad (11)$$

- the continuity of flux at the fluid lower boundary,

$$D\Theta_1\left(-\frac{1}{2}\right) = \lambda D\Theta\left(-\frac{1}{2}\right); \quad (12)$$

- the condition for surface-tension driven convection at the upper boundary,

$$D\Theta_1\left(-\frac{1}{2} - \lambda\right) = \lambda \gamma a^2 \int_{-1/2}^{1/2} \Theta dz, \quad (13)$$

where  $\lambda$  is the ratio of the thermal conductivities of the fluid and the lower boundary layer,  $K_f/K_l$ .

In order to establish the onset of convection we have to solve:

$$D = \begin{vmatrix} M_1 & M_2 \\ M_3 & M_4 \end{vmatrix} = 0, \quad (14)$$

where

$$M_4 = \begin{bmatrix} x_3 S_3 + Bi C_3 & x_1 C_1 + Bi S_1 & x_2 C_2 + Bi S_2 & x_3 C_3 + Bi S_3 \\ -\frac{(2\gamma a^2 \lambda_1) S_3}{x_1} & 0 & 0 & 0 \\ -C_3 & S_1 & S_2 & S_3 \\ \lambda_1 x_3 S_3 & -\lambda_1 C_1 & -\lambda_1 C_1 & -\lambda_1 C_1 \end{bmatrix} \quad (16)$$

$$M_1 = \begin{bmatrix} 0 & 0 & X_1 C_1 & X_2 C_2 \\ 0 & 0 & X_1 C_1 & X_2 C_2 \\ 0 & 0 & -x_1 X_1 S_1 & -x_2 X_2 S_2 \\ 0 & 0 & -x_{1m} C_1 & -x_{2m} C_2 \end{bmatrix} \quad (17)$$

$$M_2 = \begin{bmatrix} X_3 C_3 & X_1 S_1 & X_2 S_2 & X_3 S_3 \\ X_3 C_3 & -X_1 S_1 & -X_2 S_2 & -X_3 S_3 \\ -x_3 X_3 S_3 & x_1 X_1 C_1 & x_2 X_2 C_2 & x_3 X_3 C_3 \\ x_{3m} C_3 & 0 & 0 & 0 \end{bmatrix} \quad (18)$$

where  $S_i = \sinh\left(\frac{x_i}{2}\right)$ ,  $C_i = \cosh\left(\frac{x_i}{2}\right)$   $i = 1 \dots 3$ .

### 3. Simulation results

Depending on the value of the proportional gain and the lower boundary properties, the system loses stability through a real eigenvalue to stationary convection or through an imaginary eigenvalue to a time-dependent convection.

Figures 2÷4 show the bifurcation evolution for  $d_1 = 0.5$  ( $d_1$  is the relative thickness of the lower boundary layer),  $\eta = 1.0$  and  $\lambda = 1.0$ . For values of the proportional gain smaller than 41.234 the critical state correspond to a steady-state (S) convection.

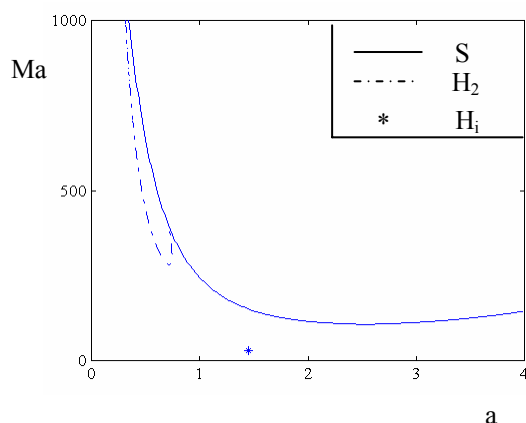


**Fig. 2.** Loss of stability toward a stationary convection (S), a time-dependent convection of ( $H_2$ ) or ( $H_i$ ) type, for  $d_1 = 1.0$ ,  $\eta = 1.0$ ,  $\lambda = 1.0$ ,  $\gamma = 41.234$ .

When  $\gamma$  is higher than 41.234, the system could lose stability toward a time dependent convection of  $H_2$  (dashed curve in Fig. 2) or isola ( $H_i$  type, the point represented in Fig. 2)

type. The isola point determines the critical state which in this case corresponds to:  $a_c = 1.45$ ,  $Ma_c = 29.3439$ ,  $\sigma_c = 8.1173$ . Consequently, for values of  $\gamma$  higher than 41.234, the onset will be towards a time-dependent ( $H_i$ ) convection.

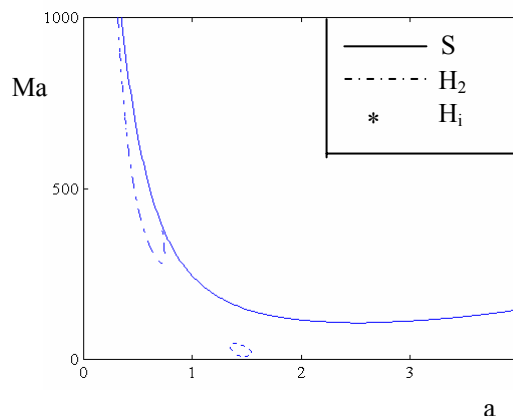


**Fig. 3.** Opening of isola point into a closed curve for  $d_1=1.0$ ,  $\eta=1.0$ ,  $\lambda=1.0$ ,  $\gamma = 41.4$ .

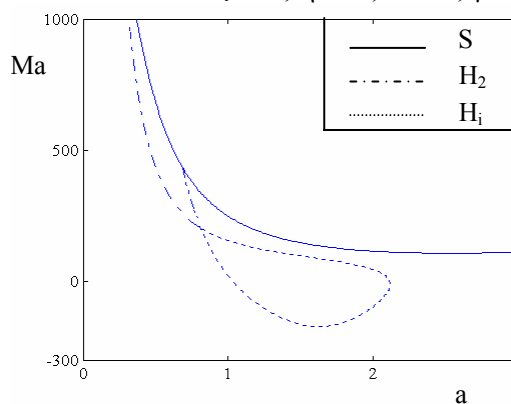
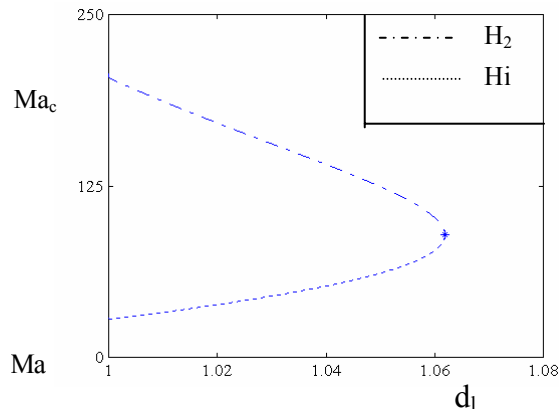


**Fig. 4.** The location of saddle point at  $a_c = 0.8045$ ,  $Ma_c = 208.7764$ ,  $\sigma = 4.3021$  and  $\gamma = 47.7200$  for  $d_1 = 1.0$ ,  $\eta = 1.0$ ,  $\lambda = 1.0$ .

Increasing the proportional gain, the S curve moves towards higher values of Marangoni number while the  $H_2$  curve shifts downward. Isola point evolves towards a closed curve  $H_i$ . The state corresponding to the minimum Marangoni number of  $H_i$  curve is now the critical state. Fig.3 illustrates its evolution for  $\gamma = 41.4$ . Continuing to increase the proportional gain, the  $H_2$  and  $H_i$  curves meet at a saddle point. This is illustrated in Fig. 4 for  $\gamma = 47.7200$ . The saddle point, for this case corresponds to:  $a_c = 0.8045$ ,  $Ma_c = 208.7764$ ,  $\sigma_c = 4.3021$ .

The existence and/or co-existence of isola and saddle points depends on the lower boundary physical and thermal properties (thickness, thermal conductivities, thermal diffusivities). Depending on the values of these parameters  $H_2$  and/or  $H_i$  curves cannot exist.

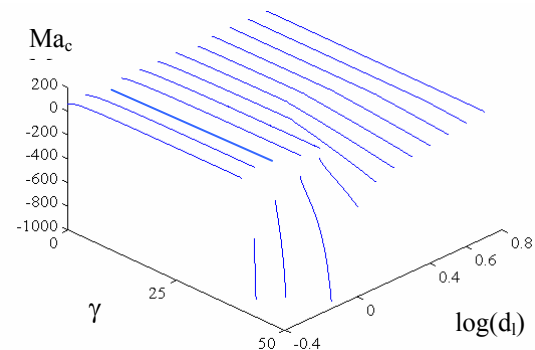
### 3.1 The influence of the lower boundary thickness



**Fig. 5.** The dependence of critical Marangoni number of isola and saddle points on the lower boundary thickness. The intersection point has the parameters  $a_c = 1.1401$ ,  $Ma_c = 89.3929$ ,  $\sigma_c = 5.676832$ ,  $\gamma = 39.8052$ ,  $d_l = 1.0618$ ,  $\eta = 1.0$ ,  $\lambda = 1.0$ .

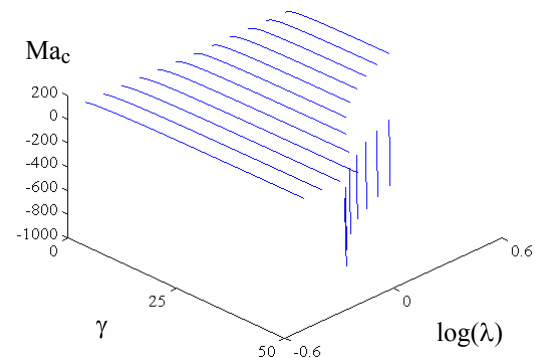
The lower boundary thickness has a critical influence on the position of critical Marangoni number in the parameters field. Figure 5 shows the evolution of Marangoni number for  $\lambda = 1.0$  and  $\eta = 1.0$  of isola and saddle points as a function of the lower boundary thickness,  $d_l$ . There is a point where isola and saddle point coincide. For our example it corresponds to:  $a_c = 1.1401$ ,  $Ma_c = 89.3929$ ,  $\sigma_c = 5.6768$ ,  $\gamma = 39.8052$  and  $d_l = 1.0618$ . For values of lower boundary thickness above that point, the loss of stability through the appearance of an isola cannot occur. This implies that smaller values of boundary thickness are desirable as they shift the onset of convection towards higher values of Marangoni number. As the boundary layer thickness increases, the loss of stability meets an  $S \rightarrow H_2$  transition.

Figure 6 illustrates this aspect in a plot of critical Marangoni number against the proportional gain and lower layer thickness. The plot presents the  $Ma_c$ - $\gamma$  dependence for twelve values of boundary thickness around the  $d_l = 1.0$  value. The plot considers  $\lambda = 1.0$  and  $\eta = 1.0$ . Increasing the lower boundary layer thickness, we actually increase the amount of time it takes for a change in the flux at the lower boundary to reach the fluid.



**Fig. 6.** Critical Marangoni number plotted against the proportional gain and boundary thickness for the thermal diffusivities ratio  $\eta = 1.0$  and the thermal conductivities ratio  $\lambda = 1.0$ .

### 3.2 The influence of the lower boundary thermal conductivity



**Fig. 7.** Critical Marangoni number plotted against the proportional gain and thermal conductivities ratio for the boundary thickness  $d_l = 0.5$  and the thermal diffusivities ratio  $\eta = 1.0$ .

For a lower boundary layer thickness of  $d_l = 0.5$  and  $\eta = 1.0$ , we plotted the dependence of critical Marangoni number-proportional gain,  $\gamma$ , for twelve values of  $\lambda$  around  $\lambda = 1.0$  value. Figure 7 presents the dependence obtained for a range of proportional gain between 1 and 50. For the lower boundary thickness considered we don't have an  $S \rightarrow H_2$  transition. The value of the proportional gain at which  $S \rightarrow H_i$  transition occurs is bigger as  $\lambda$  has smaller values. For values of  $\lambda < 1$ , an increase of lower boundary thermal conductivity leads to a slight variation of the maximum critical Marangoni number.

### 3.3 The influence of the lower boundary thermal diffusivity

For a lower layer thickness of  $d_l = 0.5$  and  $\lambda = 1.0$ , Fig. 8 presents the dependence of critical Marangoni number-proportional gain for twelve values of  $\eta$  around  $\eta = 1.0$  value and

for a range of proportional gain between 0 and 50. An increase of the thermal diffusivity of the lower boundary material leads to a shift  $S \rightarrow H_i$  transition towards higher values of the proportional gain  $\gamma$ . A higher thermal diffusivity of the lower boundary material means a faster response of the system to the influence of the control system and, consequently, higher efficiency in other words higher values for the maximum critical Marangoni number.

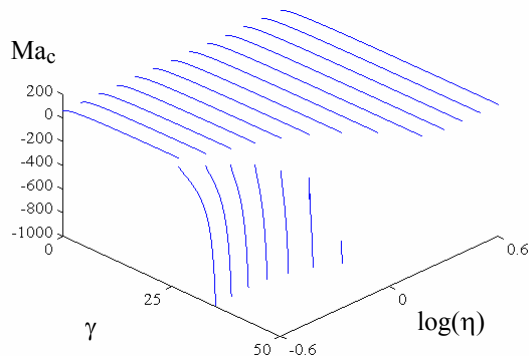


**Fig. 8.** Critical Marangoni number plotted against the proportional gain and thermal diffusivities ratio for the boundary thickness  $d_l=0.5$  and the thermal conductivities ratio  $\lambda=1.0$ .

#### 4. Conclusions

Using the linear stability analysis, the paper studies the onset of convection of infinite fluid layers with finite lower boundary heated from below with a constant heat flux. Considering microgravity conditions for the numerical simulation, Bénard-Marangoni convection is the driven phenomenon of the pattern formation.

For a finite thickness lower boundary, the physical and thermal properties of the lower boundary are coming into play when the system loses stability through a real eigenvalue towards a steady-state convection or through an imaginary eigenvalue towards a time-dependent convection. Depending on the lower boundary layer properties, the time dependent convection can be of  $H_2$  and/or  $H_i$  type meaning a dramatic decrease of the critical Marangoni number appears at smaller values of lower boundary thickness. An increase of the maximum critical Marangoni number can be obtained increasing the boundary layer thermal conductivity till the point where it becomes higher than the thermal conductivity of the fluid or increasing the thermal diffusivity of the lower boundary.

This work shows clearly how the onset of convection in an infinite fluid layer heated from below with a constant flux can be shifted

toward higher values of Marangoni number using an active control process. It also establishes guidelines for the choice of those physical and thermal properties of the lower boundary which enhance the delay of convective state.

#### References

- [1] **J.R. Pearson**, *On convection cells induced by surface tension*, J. Fluid Mech. 4, 489 (1958).
- [2] **D.A. Nield**, *Surface tension and buoyancy effect in cellular convection*, J. Fluid Mech. 19, 341 (1964).
- [3] **L.E. Scriven, C.V. Sterling**, *On cellular convection driven by surface-tension gradients: effect of mean surface tension and surface viscosity*, J. Fluid Mech. 19, 321 (1964).
- [4] **A. Thess, S.A. Orszag**, *Surface tension driven Bénard convection at infinite Prandtl number*, J. Fluid Mech. 283, 201 (1995).
- [5] **P.C. Dauby, G. Lebon**, *Bénard-Marangoni convection in rigid rectangular containers*, J. Fluid Mech. 329, 25 (1996).
- [6] **S.H. Davis**, *Buoyancy-surface tension instability by the method of energy*, J. Fluid Mech. 39, 347 (1969).
- [7] **J.W. Scanton, L.A. Segel**, *Finite amplitude cellular convection induced by surface tension*, J. Fluid Mech. 30, 149 (1967).
- [8] **A. Cloot, G. Lebon**, *A nonlinear stability analysis of the Bénard-Marangoni problem*, J. Fluid Mech. 145, 447 (1984).
- [9] **M. Neagu**, *Active Control of Heat Transfer Stability in Material Processing*, The 11<sup>th</sup> International Symposium on Modeling, Simulation and System's Identification, Galați, 2001, pag. 315-321.
- [10] **M. Neagu, G. Frumușanu**, *Finite-difference/Galerkin method for the study of a melted material layer*, The Annals of "Dunărea de Jos" University Galați, 2001, Fascicle V, pag. 61.
- [11] **G. Venezian**, *Effect of modulation on the onset of thermal convection*, J. Fluid Mech. 35, 243 (1969).
- [12] **C. Yih and C. Li**, *Instability of unsteady flows of configurations. Part 2. Convective instability*, J. Fluid Mech. 54, 143 (1972).
- [13] **L. Howle**, *The effect of boundary properties on controlled Rayleigh-Bénard convection*, J. Fluid Mech. (manuscript).
- [14] **L.E. Howle**, *Linear stability analysis of controlled Rayleigh-Bénard convection using shadowgraph measurements*, Phys. Fluids, manuscript (1997).
- [15] **L.E. Howle**, *Control of Bénard-Marangoni convection in a small aspect ratio container*, Int. J. Heat Mass Transfer 40, 817 (1997).
- [16] **L.E. Howle**, *Active control of Rayleigh-Bénard convection*, Phys. Fluids 9, 1861 (1997).
- [17] **J. Tang, H.H. Bau**, *Stabilization of the no-motion state of a horizontal fluid layer heated from below with Joule heating*, J. of Heat Trans. 117, 329 (1995).
- [18] **M. Gad-el-Hak**, *Modern developments in flow control*, Appl. Mech. Rev. 49, 365 (1996).
- [19] **S. Chandrasekhar**, *Hydrodynamic and Hydromagnetic Stability* (Dover, New York, 1981).
- [20] **M. Kubicek, M. Marek**, *Computational methods in bifurcation theory and dissipative structures* (Springer Verlag, 1984).
- [21] **E.L. Koschmieder, D.W. Switzer**, *The wave number of supercritical surface-tension-driven Bénard convection*, J. Fluid Mech. 240, 533 (1992).
- [22] **H.J. Palmer, J.C. Berg**, *Convective instability in liquid pools heated from below*, J. Fluid Mech. 97, 779 (1997).

**Controlul Activ al Convecției unui Strat de Material Topit  
II. Convecția cu Strat Limită Finit**

**REZUMAT**

*Acestă lucrare este partea a doua a unui studiu asupra controlului activ al convecției Bénard-Marangoni într-un strat de fluid infinit cu un strat limită finit. Metoda de control utilizată modifică fluxul termic proporțional cu amplitudinea aparatului de măsură. Influența proprietăților stratului limită (grosime, conductivitate și difuzivitate termică) asupra procesului de control activ este analizată. Noutatea acestui studiu constă în apariția unui punct izolat, pentru anumite domenii ale parametrilor, ca bifurcație către convecția variabilă în timp.*

**Aktive Steuerung der Konvektion in einem  
geschmolzenen materiellen Layer  
II. Konvektion mit einer begrenzten niedrigeren Grenze**

**AUSZUG**

*Dieses Papier ist das zweite Teil einer Studie der aktiven Steuerung von Bénard-Marangoni Konvektion einer endlosen flüssigen Schicht mit einer begrenzten niedrigeren Grenze, die vom Gebrüll mit einem konstanten Hitzefluß geheizt wird. Eine lineare proportionale Steuer methode wird verwendet, um den niedrigeren Grenzhitze fluß zu stören, der zum lokalen Umfang eines Shadowgraphmaßes proportional ist. Der Einfluß der Grenzschichteigenschaften (Stärke, Wärmeleitfähigkeit, Temperaturleitvermögen) auf den aktiven Steuerprozeß wird analysiert. Eine große Neuheit dieser Studie ist das Aussehen eines isola, für eine bestimmte Strecke der Prozeßparameter, als Primärgabelung in Richtung zu einer zeitabhängigen Konvektion.*